Received: March 25, 2025. Revised: April 22, 2025.

INASS

International Journal of
Intelligent Engineering & Systems

http://www.inass.org/

A Miniaturized Horizontally Oriented MIMO Antenna for 5G and Wireless Communication Systems

Nazrin Haziq Jemaludin[1] Muhannad K. Abdulhameed[2,3] Omaima Benkhadda[4]
Ahmed Jamal Abdullah Al-Gburi[1]* Dunya Zeki Mohammed[5] Tale Saeidi[6] Zahriladha Zakaria[1]

[1]Center for Telecommunication Research & Innovation (CeTRI),
Fakulti Teknologi Dan Kejuruteraan Elektronik Dan Komputer (FTKEK),
Universiti Teknikal Malaysia Melaka (UTeM), Jalan Hang Tuah Jaya, 76100, Durian Tunggal, Melaka, Malaysia
[2]Computer Scince Department, University of Kerbala, Karbala, Iraq
[3]Air Conditioning Engineering Department, Faculty of Engineering, Warith Al-Anbiyaa University, Iraq
[4]Laboratory of Mathematics, Computer Science, Electrical Engineering and Physics, EMSI-Marrakech, Morocco
[5]Department of Electronic and Communications Engineering, Gilgamesh University, Baghdad, Iraq
[6]WiSAR Lab, Atlantic Technological University (ATU), Letterkenny, Co. Donegal F92 FC93, Ireland
* Corresponding author's Email: ahmedjamal@ieee.org

Abstract: The paper introduces a novel compact MIMO antenna specifically engineered for emerging 5G and satellite communication applications. The antenna operates efficiently at 3.5 GHz and 15.6 GHz. Its primary advantage lies in its dual-band capability, achieved through a uniquely designed antenna geometry that enhances inter-element isolation and reduces return loss, all within a highly compact form factor. The proposed antenna features a miniaturized structure with dimensions of 26 × 10 × 1.6 mm³ ($0.3\lambda_o \times 0.12\lambda_o \times 0.02\lambda_o$), where λ_o denotes the wavelength at 3.5 GHz—marking a significant improvement over conventional models. The substrate, precisely optimized using CST simulation tools, possesses a low loss tangent of 0.025 and a relative permittivity of 4.3. A prototype of the antenna was fabricated and exhibits omnidirectional radiation characteristics, with peak gain values of –2.6 dBi and 3.04 dBi. Key MIMO performance metrics—including the Envelope Correlation Coefficient (ECC), Mean Effective Gain (MEG), and Diversity Gain (DG)—were evaluated through comprehensive simulations and experimental measurements. A comparative analysis with existing designs highlights the proposed antenna's superior performance and reliability.

Keywords: Multiple-input and multiple-output **(**MIMO), Wireless communication, 5G, Patch antenna, Multi-band.

1. Introduction

MIMO (Multiple-Input Multiple-Output) antenna systems have significantly advanced in recent years due to their ability to deliver higher data speeds and enhanced reliability. As a result, they have become an essential component of modern wireless technologies, including Wi-Fi, fifth-generation (5G), and Long-Term Evolution (LTE). MIMO antennas enable high-speed communication by increasing the capacity and efficiency of radio networks through multiple transmitting and receiving elements [1, 2]. MIMO antennas offer the benefit of delivering high isolation and broad bandwidth, making them well-suited for effective communication in 5G systems [3]. MIMO technology was initially explored as a broadcasting technique in 1993. Over the years, this innovative approach has been adopted across various fields [4]. MIMO enhances detection accuracy and reduces interference in radar and imaging systems, enabling more precise target identification. Similarly, in satellite communication systems, it improves signal reliability and increases data transfer rates.

The accelerated advancement of wireless communication technologies has generated an

extraordinary demand for high-performance antennas, particularly for 5G networks and future generations. The need for compact, efficient, and scalable antennas has become increasingly critical as mobile devices play an ever more integral role in daily life [5, 6]. Most modern smartphones now support 5G networks, offering enhanced bandwidth, reduced latency, and faster speeds to enable seamless voice calls and mobile data services, effectively meeting the demands of everyday communication [7]. MIMO systems use multiband antennas to reduce the need for multiple antennas while ensuring comprehensive coverage across a wide range of wireless applications. Furthermore, depending on their bandwidth properties, MIMO antennas can be classified as either wideband or multiband [8].

With the growing demand for high-performance and compact communication solutions, the significance of patch antennas in smartphone design has increased. As mobile devices evolve to accommodate cutting-edge technologies such as 5G, integrating antennas that deliver superior performance within constrained spatial dimensions has become a critical design challenge [9]. Microstrip antennas, often integrated with printed circuit boards (PCBs), are widely used due to their slim and lightweight design. However, optimizing key performance metrics—including bandwidth, gain, and efficiency—while maintaining compact size presents significant engineering challenges. Patch antennas offer notable advantages, such as their low-profile and lightweight structure, yet they also face technical hurdles, including impedance matching, bandwidth optimization, and radiation efficiency. To ensure robust connectivity without compromising a device's aesthetics or operational performance, manufacturers must overcome these challenges and strike a balance between functionality and miniaturization [10, 11]. This paper explores recent advancements in patch antenna technology, highlighting sophisticated design strategies that enable seamless integration into modern smartphones while addressing these critical challenges.

In [12], a monopole antenna is introduced that operates in a single band (3.5 GHz WiMAX) when inactive. The antenna's efficiency, measured at 86%, 93.5%, and 84.4% at 2.45 GHz, 3.5 GHz, and 5.2 GHz, respectively, demonstrates its effectiveness across these frequency ranges. Additionally, its directivity values of 2.13 dBi, 2.77 dBi, and 3.99 dBi further validate its performance An eight-port MIMO antenna, specifically designed for 5G handsets, is introduced in [13]. This antenna achieves mutual coupling values of -20 dB in the lower band and -22 dB in the upper band when operating at 3.5 GHz and 5.5 GHz. The radiation efficiency of each antenna element exceeds 68% in the lower band and 78% in the upper band, with an ECC below 0.11. In [14], a "3"-shaped monopole antenna is proposed for wireless laptop applications. This antenna resonates at 3.45 GHz and 5.5 GHz with a VSWR of less than 2. The measured impedance bandwidth for the lower band is 20% (3.21–3.91 GHz), while the upper band has a bandwidth of 15% (5.05–5.85 GHz), supporting WLAN and 5G sub-6 GHz functionality. In reference [15], a tri-band Vivaldi antenna with bandwidths of 1.6 GHz, 1.2 GHz, and 1 GHz is designed to operate at frequencies of 3.8 GHz, 5.2 GHz, and 8 GHz, respectively. A compact $40 \times 15 \times 0.8$ mm³ planar antenna for 5G terminals is presented in reference [16]. With a maximum S_{11} value of -6 dB, this antenna operates in the 700–960 MHz and 1600–5500 MHz frequency bands. Furthermore, a flexible antenna design using a PDMS substrate is described in reference [17] , achieving an impedance bandwidth of 1.225 GHz and a reflection coefficient of -37 dB. Next, author in [18] develops ASIM shape antenna achieves a bandwidth from 3.0 to 6.2 GHz, with gains between 3.3 dB and 4.2 dB, enhanced by a frequency-selective surface. In [19], author presents a capacitive-fed antenna design supports multiple modes, covering 790-6000 MHz, making it versatile for various wireless standards. Antenna in [20] combines sub-6 GHz and mmWave capabilities, allowing for efficient use of space within smartphones while maintaining performance across multiple frequency bands. Lastly, researchers in [21] discusses a single-patch antenna designed for 3.5 GHz, suitable for 5G applications and it utilizes the DGS structure to enhance bandwidth from 105.1 MHz to 158.4 MHz.

This research presents a new compact MIMO patch antenna with robust characteristics, including multiband functionality, optimized radiation patterns, and a unique geometric configuration. The suggested antenna is ideal for implementation into compact electrical devices, offering remarkable versatility for applications such as 5G, Ku-band, and K-band technologies. The antenna offers a wide bandwidth and operates within two critical frequency ranges: 3.36–3.67 GHz, with a resonant frequency at 3.5 GHz, and 15.6–20 GHz. Its exceptional performance at 3.5 GHz and 17 GHz makes it adaptable for various applications, including Ku-band, K-band, and 5G networks. Simulation results confirm the system's efficiency,

demonstrating strong performance in gain, radiation patterns, and reflection coefficients across these frequencies. To evaluate diversity performance, ECC, DG, and MEG metrics are implemented. The ECC values remain consistently below 0.1 (determined by far-field magnitudes), while the MEG for both terminals is less than -3 dB, indicating suitability for multi-standard mobile and wireless communication systems. With its compact size and frequency flexibility, the proposed antenna is an attractive option for various 5G and wireless communication applications.

The paper is organized as follows. Section 2 explains the antenna design methodology, including key parameters and substrate characteristics. Section 3 discusses the evolution of the single-antenna configuration and provides a compactness analysis. Section 4 presents the two-port MIMO antenna configuration. Section 5 examines the radiation patterns across various frequencies. Section 6 evaluates diversity performance using metrics such as ECC, DG, and MEG. Section 7 compares the proposed design with existing antennas, and Section 8 concludes the paper with key findings and suggestions for future work.

2. Antenna design methodology

In this research, the antenna is designed to operate at its most effective in the Ku and K-band frequency ranges, as well as at 3.5 GHz, which are essential for 5G communication systems. It also features a rectangular patch design. To create a super-miniaturized multiband antenna, the developed radiating patch is structured around rectangular radiators. The antenna's feed line consists of a linearly tapered transmission line with low-impedance rectangular outer surfaces that gradually transition to a specific high-impedance level. A compact multiband antenna is built on an FR4 laminate substrate with a thickness of 1.6 mm,

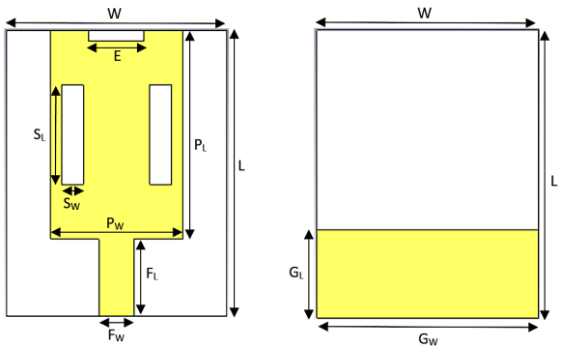

(a) (b)

Figure. 1: (a) Top and (b) Back views of the proposed multiband antenna

Table 1 Design specifications of the antenna

Variables	Dimensions (mm)	Variables	Dimensions (mm)
Substrate Length, L	13	Ground Length, GL	4
Substrate Width, W	10	Ground Width, GW	10
Patch Length, PL	9.5	Rectangular Upper Slot, E	2.5
Patch Width, PW	6	Slot Length, SL	4.5
Feedline Length, FL	3.5	Slot Length, SW	1
Feedline Width, FW	1.6	Substrate Length, L	13

a relative permittivity of 4.3, and a loss tangent of 0.02. The dimensional layout of the proposed design is shown in Fig. 1 (a), while its side view is depicted in Fig. 1 (b). A thorough examination of the dimensional requirements for the proposed multiband antenna is given in Table 1.

The substrate characteristics and the resonant frequency determine the patch dimensions. The equations presented in Eq. (1) and (2) from [22] can be applied to determine the width and length of the patch:

$$W = \frac{C}{2f_o}\sqrt{\frac{2}{\mathcal{E}_r + 1}} \tag{1}$$

$$L = \frac{C}{2f_o}\sqrt{\frac{2}{\mathcal{E}_r - 1}} \tag{2}$$

This equation defines the speed of light as C, the operating frequency as f_o, and the permittivity value of the substrate as $\mathcal{E}_r$. The width of the feedline is primarily determined by the characteristic impedance of the transmission line, which is typically set at 50 Ω. The feedline width can be calculated using the formula provided in Eq. (3) from [22]:

$$W_F = \frac{2hZ_o}{\mathcal{E}_r + 1} \tag{3}$$

The permittivity value of the substrate is denoted by $\mathcal{E}_r$. The transmission line's characteristic

impedance is denoted by Z_o. In this context, h refers to the thickness of the substrate. The antenna undergoes simulations during the design phase using CST software to refine several parameters.

2.1 Single antenna design evolution and compactness calculation

The primary configuration of the antenna design that has been proposed is a rectangular patch that is placed to a partial ground plane. We select a rectangular patch with a width of 6 mm and a length of 9.5 mm during the initial design phase.

By lowering the ground plane, introducing two symmetrical rectangular slots at the center, and positioning a horizontal slot at the top of the patch, the standard rectangular patch is modified to operate within the 3.5 GHz and 15-20 GHz range, which encompasses the sub-6 GHz, Ku, and K bands. As illustrated in Stage 1 of Fig. 2, the initial design of the traditional rectangular patch antenna is to resonate at 8 GHz on a FR-4 substrate.

Calculations have been performed to determine the patch dimensions required for the antenna to function at 8 GHz and 18 GHz in Stage 1. A rectangular metal conductor patch, measuring 6 mm × 9.5 mm, is positioned on a 10 mm × 13 mm FR4 substrate, shown in grey. As shown in Fig. 2, the resonance frequency is around 7.5 GHz, and the return loss is about 14 dB.

The four separate stages of the antenna design's development are shown in Fig. 2. The initial design, featuring a basic feed structure and a simple rectangular patch, is shown in Stage 1. The reflection coefficient curve (red line) exhibits a significant drop below -10 dB, indicating that this design primarily supports a single resonant frequency at approximately 7.5 GHz. However, its bandwidth is narrow, and it is unable to effectively accommodate higher frequencies.

The design is modified in Stage 2 to improve bandwidth by incorporating a lower ground structure. A resonance at 3.5 GHz appears, while the reflection coefficient curve (purple line) also displays an additional weak resonance near 17 GHz. Although high-er-frequency performance remains underdeveloped, these improvements mark the beginning of multi-band functionality.

Stage 3 introduces slots into the patch, significantly improving the performance of antenna across multiple frequencies. The return loss curve (blue line) now demonstrates stable resonances at 3.5 GHz, 17 GHz, and 19 GHz, all with reflection coefficients at or below -10 dB. These modifications,

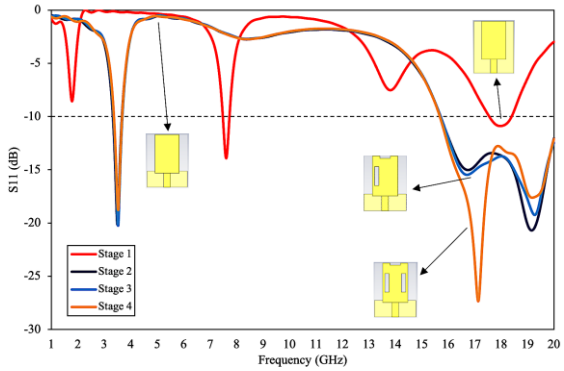

Figure. 2 Evolution of sub-6GHz, Ku and K band antenna and their reflection coefficient curves

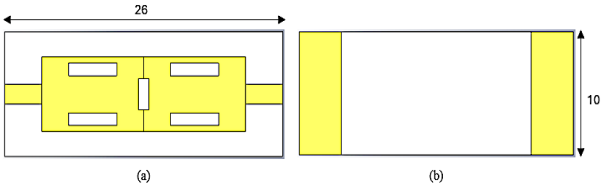

Figure. 3 MIMO antenna configuration: (a) Top layout and (b) Bottom layout

facilitated by the enhanced current distribution from the slots, enable efficient operation across sub-6 GHz, Ku band, and K band frequencies.

Finally, in Stage 4, the design is optimized for multi-band operation through the addition of more slots and further structural refinements. The reflection coefficient curve (black dashed line) reveals resonances at 3.5 GHz, 17 GHz, 19 GHz, and beyond, all of which show reduced reflection losses and strong impedance matching. All the desired resonating frequencies with excellent impedance matching have been successfully achieved. In addition to the 3.5 GHz range, these frequencies include 15.6–20 GHz. The 3.5 GHz resonant frequency also effectively covers the required 100 MHz channel bandwidth. Due to its noteworthy multiband achievement, the antenna is ideal for sub-6 GHz, Ku-band, and K-band applications.

2.2 Two port antenna

The 2 × 2 MIMO antenna structure shown is well-suited for modern wireless applications, such as 5G, due to its compact dimensions of 26 × 10 × 1.6 mm³. It comprises two identical antenna elements arranged in an anti-parallel configuration to minimize signal interference and enhance isolation. The rectangular slots are designed to optimize performance by achieving targeted resonance frequencies, while the yellow regions represent the conductive material. Fig. 3 illustrates the refined 2-element MIMO design.

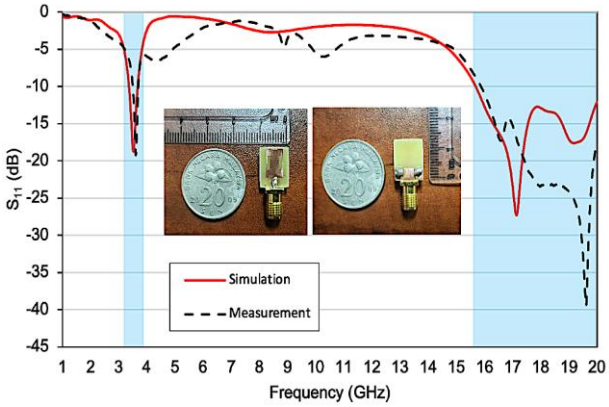

Figure. 4 Simulated and measured S11 (dB) characteristics of the proposed antenna across the frequency spectrum

3. Simulated and measured results of single antenna

CST software, an electromagnetic (EM) simulation software, was used to perform all simulations of the proposed antenna. Fig. 4 presents a comparison of the simulated and measured $|S_{11}|$ results, with measurements conducted using a VNA. According to the simulations results, the antenna exhibits high resonance and a wide impedance bandwidth (IBW) with a notable decrease in the reflection coefficient at 3.5 GHz. However, the measured results show a slight deviation in the resonance frequency. Additionally, extra rejection bands are observed at frequencies above 16 GHz, characterized by additional peaks. Fabrication tolerances, material characteristics, or irregularities in the measurement equipment are probably the causes of these differences between the simulated and measured results.

4. Two Port MIMO simulation and measurement results

The fabricated prototype of a compact two-port MIMO antenna is shown in Fig. 5. The antenna comprises two identical radiating elements arranged in an opposing configuration, enhancing isolation performance. The antenna is constructed on a 1.6 mm thick FR-4 substrate and incorporates SMA connectors to enable accurate measurement validation. To highlight its compact dimensions, the fabricated prototype is shown alongside a 50-sen Malaysian coin, demonstrating its suitability for space-constrained applications, such as smartphones. The decoupling structure achieves a measured isolation of at least –22 dB, with values reaching beyond –33 dB. The proposed MIMO radiator has physical dimensions of 0.45λl × 0.45λl and is

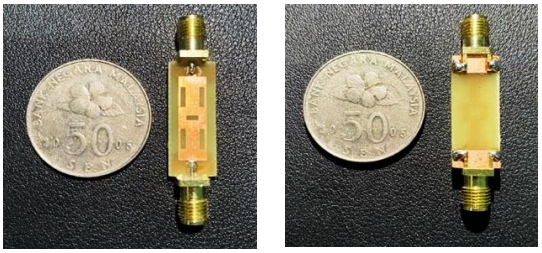

Figure. 5 MIMO Antenna prototype

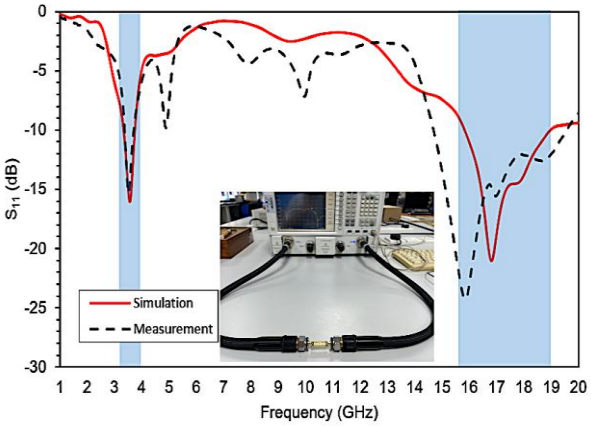

Fig. 6 Measured and simulated MIMO antenna reflection coefficient

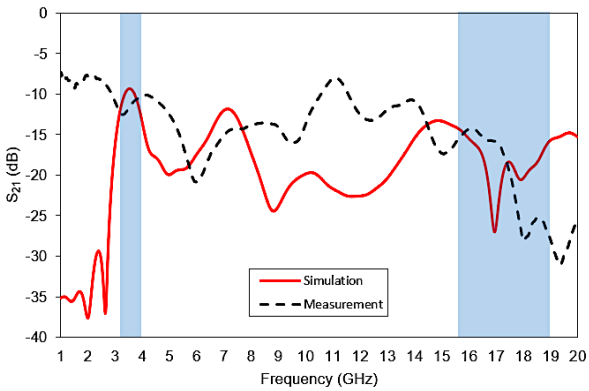

Fig. 7 Measured and simulated MIMO antenna transmission coefficient.

fabricated on an FR-4 substrate with a thickness of 1.6 mm.

The impedance matching and isolation properties of the MIMO antenna are depicted in Figs. 6 and 7, showcasing the measured and simulated reflection coefficients (S_{11} and S_{22}) as well as the transmission coefficients (S_{21} and S_{12}). Fig. 6 depicts a broad impedance bandwidth with distinct resonance dips, indicating effective impedance matching at specific frequencies. While the simulated S_{11} and S_{22} curves exhibit a similar trend, the measured results show minor discrepancies, likely due to fabrication tolerances, connector mismatches, or variations in the measurement setup.

Despite these variations, the simulated and measured results roughly match, showing that the antenna maintains consistent impedance matching over the frequency range.

Fig. 7 illustrates the mutual coupling between antenna elements by presenting the simulated and measured transmission coefficients (S_{21} and S_{12}). The measured S_{21} exhibits fluctuations and increased attenuation at specific frequencies, whereas the simulated S_{21} remains relatively stable, suggesting the influence of mutual coupling effects, fabrication inaccuracies, or external interference.

Overall, the MIMO antenna design improves overall bandwidth and enhances multi-frequency performance compared to a single-element antenna, while maintaining robust impedance matching at the primary band (3.5 GHz). However, the observed deviations in the measured results indicate that its performance is marginally affected by fabrication tolerances, mutual coupling, and measurement inconsistencies.

Simulated gain and radiation efficiency curves are shown in Fig. 8, which shows that the antenna achieves a peak gain of 3.5 dB and an efficiency between 6% and 70% across its operational frequency range.

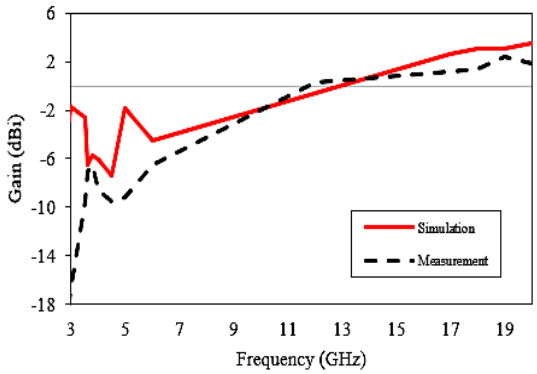

(a)

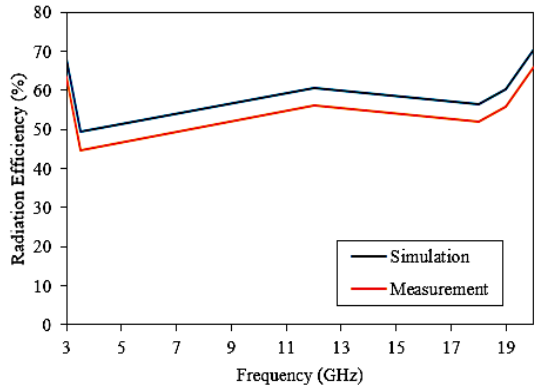

(b)

Figure. 8 Simulated and measured: (a) gain, (b) radiation efficiency

5. Radiation pattern of two port MIMO

Fig. 9 compares the simulated and measured results at 3.5 GHz and 17 GHz to show the proposed antenna's 2D radiation patterns. The radiation pattern at 3.5 GHz is shown in Fig. 9 (a), which is distinguished by a dipole-like arrangement and good agreement between modelling and experiment. This alignment indicates effective impedance matching and high radiation efficiency. In contrast, Fig. 9 (b) depicts the radiation pattern at 17 GHz, which becomes increasingly complex as higher-order modes are excited, leading to the formation of additional bands. While discrepancies between simulated and measured results are noticeable, particularly at 17 GHz, these variations may be attributed to measurement equipment limitations, material inconsistencies, or fabrication tolerances. The measured outcomes validate the antenna's radiation performance throughout the frequency range by typically matching the general trend of the predicted patterns. Using the experimental configuration depicted in Fig. 10, the radiation pattern was measured.

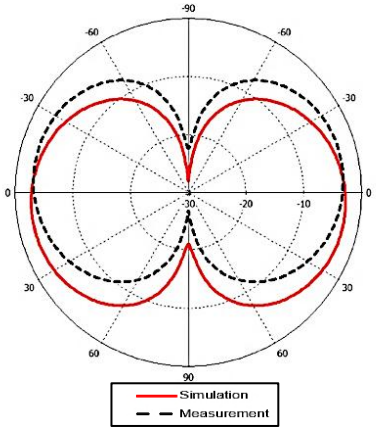

(a)

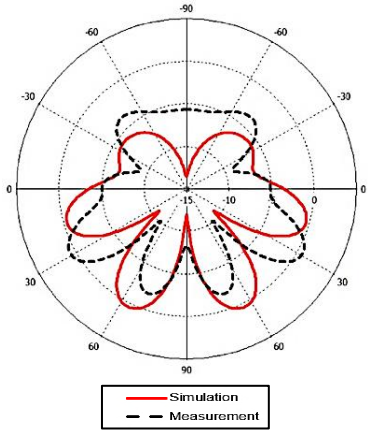

(b)

Figure. 9 The proposed antenna's radiation pattern at: (a) 3.5 GHz and (b) 17 GHz

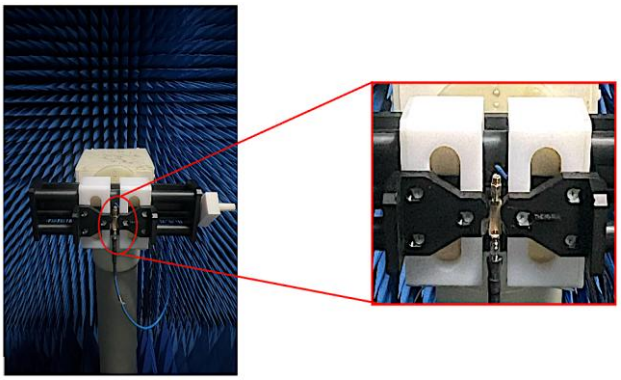

Figure. 10 Antenna radiation pattern measurement setup

6. Diversity performance of two port MIMO

The ECC, DG, MEG, and CCL are major diversity metrics that are used to evaluate a MIMO antenna's performance. According to [23], a crucial characteristic of the MIMO radiator is its low terminal-to-terminal mutual coupling, as measured by metrics like DG and ECC.

Fig. 11 shows the ECC for the proposed antenna as an indicator of frequency. Optimal MIMO performance is ensured by the simulated ECC, which remains below 0.5 across most of the operating band, indicating minimal signal correlation between antenna elements. However, at certain frequency points, the ECC exceeds 0.5, suggesting the presence of mutual coupling effects. The ECC can be determined using the scattering parameters of individual MIMO elements, as expressed by the following equation [24]:

$$ECC = \frac{|S_{11}^{*}S_{12} + S_{21}^{*}S_{22}|^2}{(1-|S_{11}|^2-|S_{21}|^2)(1-|S_{22}|^2-|S_{12}|^2)} \quad (4)$$

Fig. 12 presents the Diversity Gain (DG) across the relevant frequency spectrum, where simulated DG values consistently exceed 9.9 dB, indicating strong diversity performance. Since DG is inversely related to ECC, variations in ECC correspond to fluctuations in DG. According to the results, the suggested MIMO antenna exhibits significant diversity gain, which is essential for improving the dependability and capability of MIMO systems by guaranteeing efficient signal decorrelation. The Diversity Gain (DG) value can be derived using the formula provided in [25]:

$$DG = 10\sqrt{1-ECC^2} \quad (5)$$

The MEG, which measures the ratio of the power received by the antenna to the overall average power of the isotropic radiator's reception of horizontally and vertically polarised waves, is depicted in Fig. 13. The results show that MEG remains below -3 dB across the entire operating band, within the acceptable range of -3 dB ≤ MEG ≤ -12 dB. The Mean Effective Gain (MEG) for a MIMO antenna system can be calculated using the equation provided in [25]:

$$MEG = 0.5\mu_{ir} = 0.5\left[1-\sum_{j=1}^{l}(S_{ij})\right] \quad (6)$$

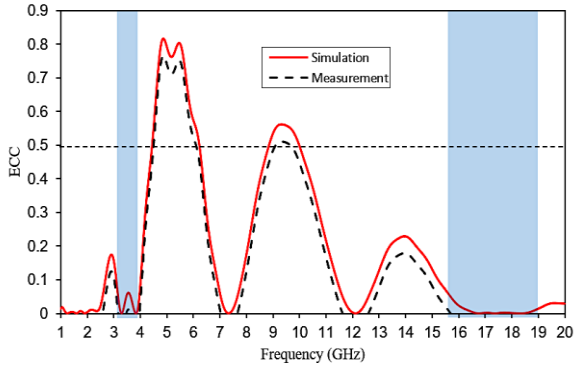

Figure. 11 Simulated and measured ECC for proposed antenna

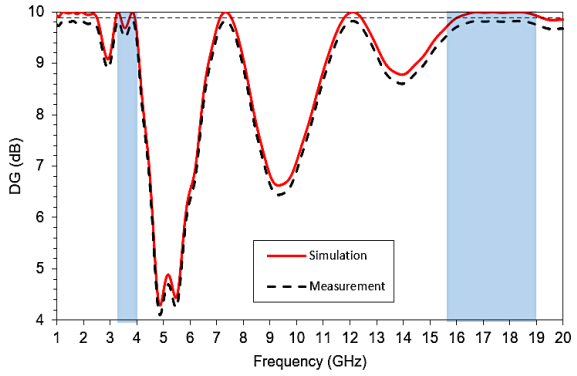

Figure. 12 Simulated and measured DG for proposed antenna

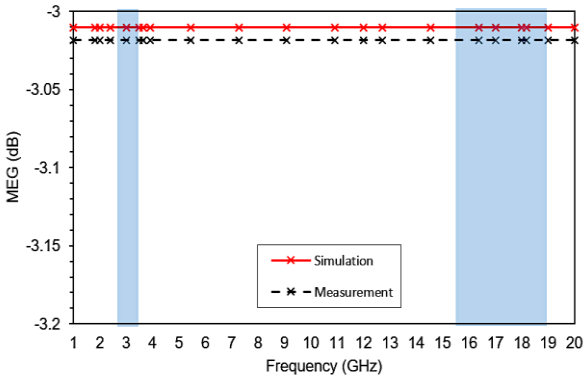

Fig. 13 Simulated and measured MEG for proposed antenna

Table 2 Comparison for various related works

Ref	Operating Frequency (GHz)	Antenna Size (mm^3)	Substrate Type	Return Loss S11	Gain (dBi)
[12]	2.45 3.5 5.2	40 × 35 × 1.6	FR-4	-15 -27 -14	1.48 3.26 2.47
[13]	3.5 5.5	140 × 70 × 6	FR-4	-23 -28	2.8 3.2
[14]	3.45 5.5	17.5 × 6 × 0.2	-	-24 -17	5.3 5.25
[15]	3.8 5.2 8	24.8 × 40 × 0.254	Rogers 5880	-18 -21 -22	6.75
[16]	0.7-0.96 1.6-5.5	40 × 15 × 0.8	FR-4	-23 -30	1.66 4.72
[17]	6.2	20 × 15 × 1.6	FR-4	-38	3.5
[18]	3.2-6.8	30 × 35 × 1.6	FR-4	-42	-
[19]	0.7-6	80 × 5 × 4.5	-	-	-
[20]	0.68-1 1.68-3 23.3-30.8	6.5 × 1.51 × 1.2	Rogers RO4350B	- - -40	-
[21]	3.5	40 × 52 × 1.2	FR-4	-39	3.16
This work	3.5 17	13 × 10 × 1.6	FR-4	-19 -39	3.5

7. Comprehensive evaluation of recent pioneering research

Key factors, including dimensions, frequency bands, substrate materials, and return loss, are evaluated in Table 2, where the authors compare the sub-6 GHz, K, and Ku-band antenna design with existing comparable antennas (S_{11}). The proposed antenna exhibits superior radiation performance and remarkable compactness, making it ideal for 5G mobile devices.

8. Conclusion

This study presents a compact, multi-band MIMO microstrip patch antenna specifically designed for 5G applications. It demonstrates efficient performance across the sub-6 GHz, Ku, and K-band frequency ranges. Fabricated on an FR4 substrate, the antenna is optimized to resonate at 3.5 GHz and 17 GHz, covering the 3.3–3.6 GHz and 14.5–20 GHz bands. It exhibits excellent return loss, with measured results closely matching simulations. MIMO performance is validated by a balanced mean effective gain (MEG) and a low envelope correlation coefficient (ECC). Its effectiveness is further supported by omnidirectional radiation and peak gain values of –2.6 dBi and 3.04 dBi. While this work focuses on laboratory validation and electromagnetic simulations, we acknowledge that real-world performance may be affected by factors such as multipath propagation and physical obstructions. Future work will involve evaluating the antenna in practical deployment scenarios and exploring enhancement strategies, including reconfigurable architectures, diversity techniques, and optimized placement. In conclusion, the proposed antenna offers a compact, adaptable, and high-performance solution for modern 5G MIMO communication systems.

Conflicts of Interest

The authors declare no conflict of interest.

Author Contributions

Conceptualization, A.J.A. Al-Gburi and N.H. Jemaludin; methodology, N.H. Jemaludin and A.J.A. Al-Gburi; software, N.H. Jemaludin and D.Z. Mohammed; validation, A.J.A. Al-Gburi, O. Benkhadda, and Z. Zakaria; formal analysis, A.J.A. Al-Gburi and M.K. Abdulhameed; investigation, N.H. Jemaludin; resources, Z. Zakaria and M.K. Abdulhameed; data curation, D.Z. Mohammed; writing—original draft preparation, N.H. Jemaludin; writing—review and editing, O. Benkhadda, A.J.A. Al-Gburi and T. Saeidi; visualization, D.Z. Mohammed; supervision, A.J.A. Al-Gburi; project administration, A.J.A. Al-Gburi; funding acquisition, O. Benkhadda.

Acknowledgments

The authors would like to thank Universiti Teknikal Malaysia Melaka (UTeM) and the Ministry of Higher Education (MOHE) of Malaysia for supporting this project.

References

[1] A. Reha, O. Benkhadda, A. O. Said, A. El Amri, and A. J. A. Al-Gburi, "Design of Sub-6GHz and Sub-7GHz Dragon Fractal Antenna for 5G Applications with Enhanced Bandwidth", *Int. J. Intell. Eng. Syst*., Vol. 18, No. 2, 2025, doi: 10.22266/ijies2025.0331.02.

[2] V.K.R. Devana, et al., "Design and Analysis of a Compact Four-Port MIMO Antenna with Enhanced Isolation for UWB Applications", *International Journal of Intelligent Engineering & Systems*, Vol. 18, No. 5, 2025, doi: 10.22266/ijies2025.0531.13.

[3] A. J. A. Al-Gburi, "5G MIMO Antenna: Compact Design at 28/38 GHz with Metamaterial and SAR Analysis for Mobile Phones", Przeglad Elektrotechniczny, Vol. 2024, No. 4, pp. 171-174, 2024.

[4] P. Kumar, A. K. Singh, R. Kumar, R. Sinha, S. K. Mahto, A. Choubey, and A. J. A. Al-Gburi,"High Isolated Defected Ground Structure Based Elliptical Shape Dual Element MIMO Antenna for S-Band Applications", *Progress In Electromagnetics Research C*, Vol. 143, pp. 67- 74, 2024.

[5] P. Kumar, A. K. Singh, R. Kumar, S. K. Mahto, P. Pal, R. Sinha, A. Choubey, and A. J. A. Al-Gburi, "Design and Analysis of Low Profile Stepped Feedline with Dual Circular Patch MIMO Antenna and Stub Loaded Partial Ground Plane for Wireless Applications", *Progress In Electromagnetics Research C*, Vol. 140, pp. 135-144, 2024.

[6] R. R. Elsharkawy, K. F. A. Hussein, and A. E. Farahat, "Miniaturized Multi-band Millimeter-Wave Vivaldi Antenna with Performance Optimization at 28 GHz for 5G MIMO Applications", *J Infrared Millim Terahertz Waves*, Vol. 45, No. 3–4, pp. 208–232, 2024, doi: 10.1007/s10762-024-00965-2.

[7] R. K. Mistri, S. K. Mahto, A. K. Singh, R. Sinha, A. J. A. Al-Gburi, T. A. H. Alghamdi, and M. Alathbah, "Quad Element MIMO Antenna for C, X, Ku, and Ka-Band Applications", *Sensors*, Vol. 23, No. 20, p. 8563, 2023.

[8] N. H. Jemaludin *et al.*, "A comprehensive review on MIMO antennas for 5G smartphones: Mutual coupling techniques, comparative studies, SAR analysis, and future directions", *Results in Engineering*, Vol. 23, p. 102712, 2024, doi: 10.1016/j.rineng.2024.102712.

[9] A. Ghaloua, J. Zbitou, L. Abdellaoui, M. Latrach, A. Tajmouati, and A. Errkik, "A Novel Configuration of a Miniature Printed Antenna Array Based on Defected Ground Structure", *International Journal of Intelligent Engineering and Systems*, Vol. 12, pp. 211-220, 2018, doi: 10.22266/ijies2019.0228.21.

[10] C. R. Jetti, T. Addepalli, S. R. Devireddy, G. K. Tanimki, A. J. A. Al-Gburi, Z. Zakaria, and P. Sunitha, "Design and Analysis of Modified U-Shaped Four Element MIMO Antenna for Dual-Band 5G Millimeter Wave Applications", *Micromachines*, Vol. 14, No. 8, p. 1545, 2023.

[11] R. H. Elabd and A. J. A. Al-Gburi, "Low mutual coupling miniaturized dual-band quad-port MIMO antenna array using decoupling structure for 5G smartphones", *Discov. Appl. Sci*., Vol. 6, p. 189, 2024.

[12] I. Ali Shah, S. Hayat, I. Khan, Imtiaz. Alam, S. Ullah, and A. Afridi, "A Compact, Tri-Band and 9-Shape Reconfigurable Antenna for WiFi, WiMAX and WLAN Applications", *International Journal of Wireless and Microwave Technologies*, Vol. 6, No. 5, pp. 45–53, Sep. 2016, doi: 10.5815/ijwmt.2016.05.05.

[13] A. Khan, A. Wakeel, L. Qu, and Z. Zahid, "Dual-band 8 × 8 MIMO antenna with enhanced isolation and efficiency for 5G smartphone applications", *AEU - International Journal of Electronics and Communications*, Vol. 163, p. 154600, 2023, doi: 10.1016/j.aeue.2023.154600.

[14] J. S. Kulkarni, "An ultra-thin, dual band, Sub 6 GHz, 5G and WLAN antenna for next generation laptop computers", *Circuit World*, Vol. 46, No. 4, pp. 363–370, 2020, doi: 10.1108/CW-07-2019-0076.

[15] T. Saeidi *et al.*, "High Gain Triple-Band Metamaterial-Based Antipodal Vivaldi MIMO Antenna for 5G Communications", *Micromachines (Basel)*, Vol. 12, No. 3, p. 250, Feb. 2021, doi: 10.3390/mi12030250.

[16] Z. An and M. He, "A Simple Planar Antenna for Sub-6 GHz Applications in 5G Mobile Terminals", *ACES Journal*, Vol. 35, No. 1, pp. 10-15, 2020.

[17] T. Singh, P. Sharma, S. Tripathi, and V. S. Tripathi, "Elliptical Multi-Orbital Truncated Flexible Patch Antenna Using PDMS Substrate

for Sub-6 GHz Applications", *Def Sci J*, Vol. 74, No. 4, pp. 546–551, 2024, doi: 10.14429/dsj.74.19018.

[18] S. Ara and P. K. Nunna, "ASIM Shape Wide band High-Gain Patch Antenna Integrated with Frequency-Selective Surface as Super Strate for Sub-6GHz 5G Applications", *International Journal on Recent and Innovation Trends in Computing and Communication*, Vol. 10, No. 2s, pp. 23–28, 2022, doi: 10.17762/ijritcc.v10i2s.5908.

[19] S. S. ALja'afreh, A. Khalfalla, and A. Omar, "Universal Antenna with a Small Non-Ground Portion for Smartphone Applications", *International Journal on Communications Antenna and Propagation (IRECAP)*, Vol. 9, No. 4, p. 292, 2019, doi: 10.15866/irecap.v9i4.17082.

[20] X. Xia *et al.*, "Millimeter-Wave and Sub-6 GHz Aperture-Shared Antenna and Array for Mobile Terminals Accessing 5G/6G-Enabled IoT Scenarios", *IEEE Internet Things J*, Vol. PP, p. 1, 2024, doi: 10.1109/JIOT.2024.3366701.

[21] G. Kartikasari, M. P. K. Praja, and S. Romadhona, "Design of Rectangular Patch Microstrip Antenna with Defected Ground Structure Method at 3.5 GHz Frequency for 5G Technology", *Journal of Information Technology and Its Utilization*, Vol. 6, No. 2, pp. 79–85, 2023, doi: 10.56873/jitu.6.2.5259.

[22] C. J. M. Andrews, A. S. K. Narayanan, and A. Marazhchal Sunil, "Compact Metamaterial based Antenna for 5G Applications", *Results in Engineering*, Vol. 24, 2024, doi: 10.1016/j.rineng.2024.103269.

[23] G. S. Sharma and A. Gupta, "Mutual coupling reduction of two-port dielectric resonator MIMO antenna using defected ground structure", *Int J Microw Wirel Technol*, Vol. 16, No. 6, pp. 1056–1070, 2024, doi: 10.1017/S1759078724000862.

[24] S. Angadi, Y. Sharma, N. S. Raghava, and T. Sabapathy, "A metasurface based close-proximity two-port circularly polarized MIMO antenna for mid-band sub-6 GHz 5G applications", *AEU - International Journal of Electronics and Communications*, Vol. 183, 2024, doi: 10.1016/j.aeue.2024.155379.

[25] T. Raj, R. Mishra, A. Kapoor, D. Pandey, and S. Kundu, "A compact quad port MIMO antenna with gain augmentation using angularly stable and polarization insensitive FSS for 5G communication", *AEU - International Journal of Electronics and Communications*, Vol. 190, 2025, doi: 10.1016/j.aeue.2024.155636.